STRUCTURED LIGHT SYSTEM CONFIGURATION DETERMINATION FOR EFFICIENT 3D SURFACE RECONSTRUCTION

A. DIPANDA and S. WOO
Université de Bourgogne, Laboratoire LE2I (CNRS UMR 5158), BP 47870 – 21078 DIJON CEDEX, FRANCE
adipanda@u-bourgogne.fr

ABSTRACT

This paper presents a new method for solving the correspondence problem in 3D shape reconstruction using a Structured Light System (SLS) which projects a grid of laser rays. In this particular case, the correspondence problem amounts to matching up the laser rays and the illuminated spots. We propose a strategy for obtaining Configurations Of the System –COS- (i.e. the positions of the camera, the laser projector and the measuring scene) that allow to perform an unambiguous direct correspondence. Experimental results demonstrate that our methodology provides our SLS with high capabilities, which permits an efficient use in dynamic applications.

1. INTRODUCTION

3D information of a given shape can be obtained using the active stereovision approach which utilizes a camera and an artificial source of energy that illuminates the measuring object. The simplest schemes project a single light beam [1] while the most elaborated systems, called Structured Light Systems (SLS), project a known pattern [2]. In this paper, we use an SLS which projects a grid of laser rays. An SLS object image consists of spots created by the laser rays that intersect the object. The correspondence problem in this particular case boils down to matching up the spots with the laser rays [3]. According to the Configuration Of the System –COS- (i.e. the relative positions of the camera, the laser projector and the analyzed object) the correspondence is either a very straightforward or a hard combinatorial problem. Hence, our aim is to propose a method that automatically provides COSs which allow an efficient and unambiguous direct correspondence procedure.

2. SLS DESCRIPTION AND CALIBRATION

Our SLS consists of a camera and a laser emitter which projects a pyramid shaped beam composed of 361 (19×19) rays. The angle between two consecutive rays in both the horizontal and vertical directions, is fixed and equals 0.77°. The SLS is calibrated using the method proposed in [4]. This calibration method provides the parameters needed for:

(1) *the correspondence problem*; a set of 361 segments, referred to as the *calibration segments*, is computed. Each segment approximates the projection in the image plane, of the part of a ray which crosses the *workspace*, i.e. the area within which the analyzed object must be located. The workspace is bounded by two planes Π_0 and Π_1 perpendicular to the central ray (see Fig. 1a).

(2) *the 3-D shape reconstruction*; the relationship between the curvilinear abscissa of a 2D point on a segment and the depth of its corresponding 3D point is modeled through an hyperbolic function (see Fig. 1b).

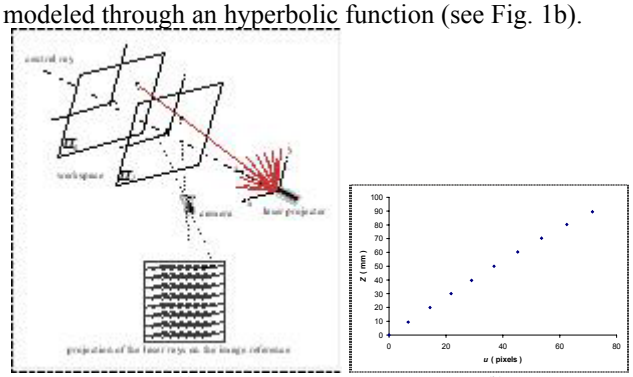

(a) (b)

Fig. 1: (a) Scheme of the system calibration process. (b) Example of a laser ray depth curve versus the curvilinear abscissa.

Once the point-segment correspondence is achieved (see section3), the Z coordinate of an illuminated 3D point is computed using the depth function described above. The other coordinates, X and Y, are obtained by:

$$X = Z \cdot \tan(\varphi_X) \quad (1a)$$

$$Y = Z \cdot \tan(\varphi_Y) \quad (1b)$$

where φ_X (resp. φ_Y) is the angle around the X-axis (resp. the Y-axis) between the central ray and the ray matched with the spot corresponding to the 3D point.

3. CORRESPONDENCE PROBLEM

The correspondence procedure uses two types of data:

(1) The calibration segments $S_{i,j(I=-9..9,j=-9..9)}$. The size and the orientation of segments depend on the COS.

(2) A set of 2D points $P=\{P_k, k=1,..M\leq 361\}$ which represent the centers of spots detected in the object image by using an image segmentation process.

The correspondence problem amounts to associating each point P_k together with one segment $S_{i,j}$. In theory, a point

may be coupled with the segment it lies on. However, in practice, many ambiguities can occur (see Fig. 2a): first, two segments can overlap (see Fig. 2b (1)), second, due to errors from segment approximation and the segmentation process, the points are not exactly on the segments; a point can be located with equivalent gaps between two very close segments (see Fig. 2b (2)-(3)). Obviously, an unambiguous direct correspondence can be achieved if neighboring segments are distant enough in both the horizontal and vertical directions. Hence, our goal is to determine COSs that produce such calibration segments.

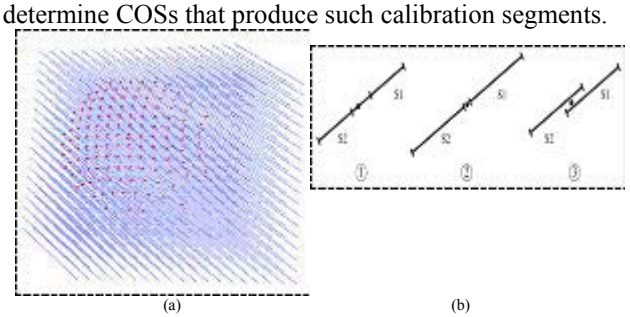

(a) (b)

Fig. 2 : (a) Calibration segments superimposed with image points; (b) Different ambiguous cases in the correspondence problem.

A COS is defined by the respective locations of the camera, the laser projector, and the workspace. Note that the distance between the workspace and the laser projector is set by the user to allow the maximum rays to intersect the analyzed object. Hence, only the position of the camera with respect to the laser projector must be determined. This is achieved in two steps: first, we model the calibration segments and second, we define the valid area for positioning the camera.

The calibration segments are modeled using an ideal camera. Let us assume that the laser projector orifice is at the origin of the world coordinate system ($OX_w, Y_w Z_w$) and that the central ray coincides with the Z_w-axis. Let p^0_{wij} and p^1_{wij} respectively be the points illuminated by the ray R_{ij} on both *workspace* boundary planes Π_0 and Π_1 (see Fig. 3a).Their coordinates are given by:

$$p^n_{wij} = \begin{bmatrix} d_n \tan(j\omega) & d_n \tan(i\omega) & d_n \end{bmatrix}^T \quad (2)$$

where d_n is the distance between the laser projector and the n^{th} plane, $n \in \{0, 1\}$ and ω is the inter-angle (0.77°).

Let $p^0_{sij} = \begin{bmatrix} x^0_{sij} & y^0_{sij} \end{bmatrix}^T$ and $p^1_{sij} = \begin{bmatrix} x^1_{sij} & y^1_{sij} \end{bmatrix}$ respectively be the projections in the image plane of $p^0_{wij} = \begin{bmatrix} x^0_{wij} & y^0_{wij} & z^0_{wij} \end{bmatrix}^T$ and $p^1_{wij} = \begin{bmatrix} x^1_{wij} & y^1_{wij} & z^1_{wij} \end{bmatrix}^T$. Using the homogeneous coordinates gives:

$$p^n_{sij} = p^n_{wij}[E][P] \quad (3)$$

where $n \in \{0, 1\}$, $[P]$ is the perspective projection matrix based on the focal length of the camera f and the field of view h and $[E]$ is the essential matrix based on the camera word coordinates (C_x, C_y, C_z).

The equations of all the segments $S_{ij} = \overline{p^0_{sij} p^1_{sij}}$ (i =-9..9 and j=-9..9) can be obtained using equat. (2) and (3). The reader can refer to [5] for more details on camera modeling.

Recall that *an unambiguous direct correspondence can be performed if the segments are well separated.* More precisely, there must be an horizontal gap Δ_x (resp. a vertical gap Δy) greater than a threshold α (resp. α') between two consecutive segments (see Fig. 3b).

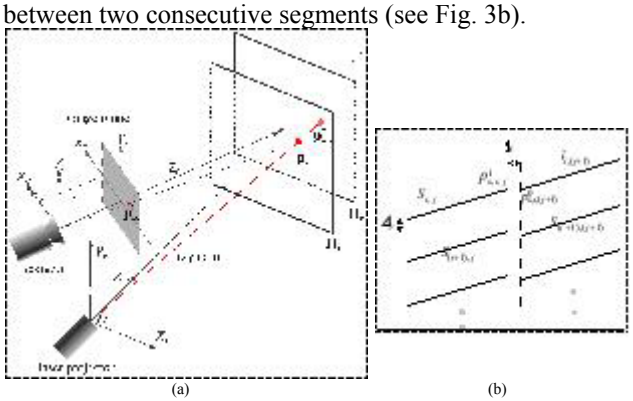

(a) (b)

Fig. 3: (a) Scheme of the calibration segment modeling. (b) Horizontal (Δ_x) and vertical (Δy) gap between two consecutive segments.

Let us first state three main properties of the SLS:

(1) Separating the segments in the horizontal and the vertical directions are two similar problems.

(2) The camera positioning problem is symmetric with respect to the plane Y_wOZ_w.

(3) If there is a gap between two consecutive segments $S_{i,j}$ and $S_{i,j+1}$, then, there is also a gap between all the consecutive segments $S_{k,j}$ and $S_{k,j+1}$ (where $k \neq i$).

For the sake of clarity, we first describe the camera positioning valid area determination, to separate the segments in the horizontal direction, within the negative half of the X_wOZ_w plane, then we extend the results to the whole space and to the vertical direction case. We propose a two-phase analysis. First, we determine the initial valid area corresponding to the case where the threshold α is equal to zero. Second, this initial valid area is utilized to extend the results to the case where α is strictly positive.

Let us assume that the origin of the laser projector, the optical center of the camera and the camera x-axis are in the X_WOZ_W plane. The rays $R_{(0,j)(j=-9,..,9)}$ lie on the X_WOZ_W plane and intersect the planes Π_1 and Π_0 on points $p^1_{w0j(j=-9,..,9)}$ and $p^0_{w0j(j=-9,..,9)}$ respectively. The projections of these points in the image plane are the respective points $p^1_{s0j(j=-9,..,9)}$ and $p^0_{s0j(j=-9,..,9)}$ which define the segments $S_{0j(j=-9,..,9)}$. Note that $S_{0j(j=-9,..,9)}$ are aligned. Now assume that the camera moves away from the laser projector (i.e. C_x decreases) and, let us consider the two leftmost rays $R_{0,-9}$ and $R_{0,-8}$ and their corresponding segments $S_{0,-9}$ and $S_{0,-8}$. As the camera moves, $S_{0,-9}$ and $S_{0,-8}$ become closer and closer and, overlap when $p^1_{s0,-9}$ and $p^0_{s0,-8}$, the respective right endpoint of $S_{0,-9}$ and left endpoint of $S_{0,-8}$ merge into a single point (see Fig. 4a (pos2)). The valid area for positioning the camera is then on the right side of

the line $l_{-9}=(P^{I}_{w0,-9},P^{0}_{w0,-8})$. By repeating the same reasoning on the consecutive segments S_{0j} and $S_{0(j+1)\ (j=-8,..8)}$, we obtain the set of lines $l_j=(P^{I}_{w0,j},P^{0}_{w0,j+1})_{(j=-8,..8)}$ (see Fig. 4b). Each line delimits an elementary valid area such that the respective consecutive segments do not overlap (i.e. α=0). And, the final valid area is the intersection of all these elementary valid areas.

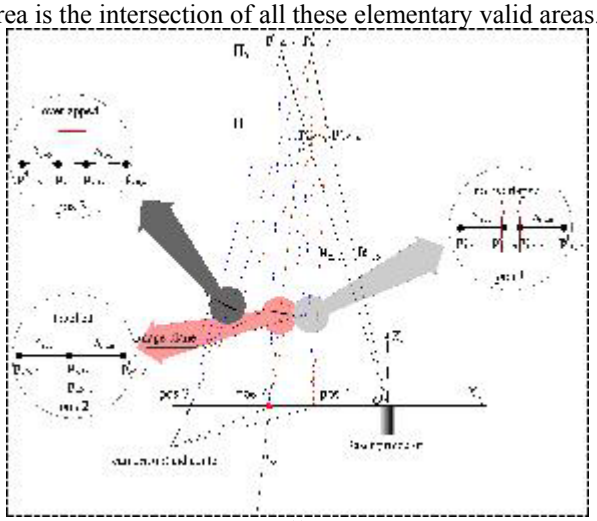

(a)

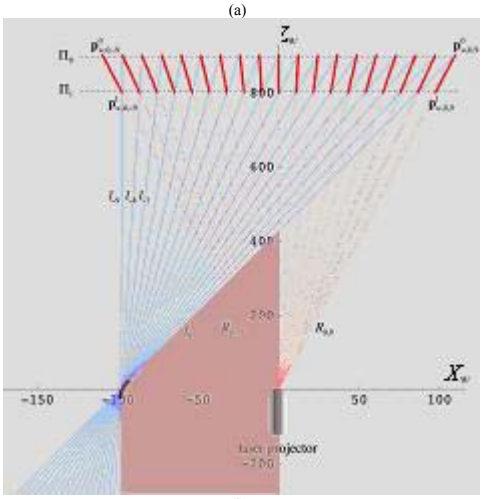

(b)

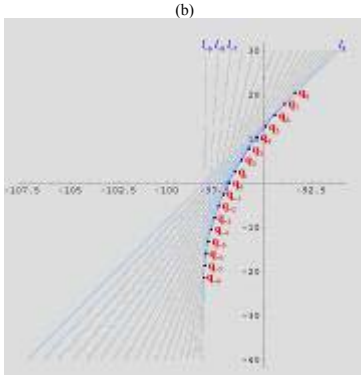

(c)

Fig. 4: (a) Illustration of the segments $S_{0,-9}$ and $S_{0,-8}$ in the image plane when the camera moves away from the laser projector. (b) Construction of the valid area. The final valid area is the shaded area. (c) Zoom of the middle part of the valid area.

For α>0, our strategy consists in substituting a new set of lines $l^{*}_{j(j=-9,..8)}$ for the set of lines $l_{j(j=-9,..8)}$. The line l^{*}_{j} is obtained as follows:

(1) position the camera on the point q_j which is the intersection between l_j and $l_{(j+1)}$ (see Fig. 4c);

(2) determine the point $P^{I*}_{w0,j}$ on the plane Π_I whose the projection $P^{I*}_{s0,j}$ in the image plane is on the segment $S_{0,(j+1)}$ such that:

$$d(P^{I}_{s0,j},P^{I*}_{s0,j})=\alpha \qquad (4)$$

(3) compute the equation of the line $l^{*}_{j}=(P^{I*}_{w0,j},P^{0}_{w0(j+1)})$.

The point $P^{I*}_{w0,j}$ presents two main advantages. First, when the camera is positioned at q_j, the coordinates $(x^{I*}_{s0,j}, y^{I*}_{s0,j})$ of its projection $P^{I*}_{s0,j}$ in the image plane can easily be calculated since the segments $S_{0,j(j=-9,..9)}$ are aligned. Second, two coordinates of $P^{I*}_{w0,j}$ are known ($y^{I*}_{w0,j}=0$ and $z^{I*}_{w0,j}=d_1$). The third coordinate $x^{I*}_{w0,j}$ is defined by:

$$P^{I*}_{s0,j}=P^{I*}_{w0,j}[E][P] \qquad (5)$$

The lines $l^{*}_{j}=(P^{I*}_{w0,j},P^{0}_{w0(j+1)})_{(j=-9,..8)}$ then obtained delimit the final valid area similarly to as the lines $l_{j(j=-9,..8)}$ delimit the initial valid area.

To summarize, the valid area in the negative half of the X_WOZ_W plane is bounded as follows :

1. In the middle part (around the X_W –axis) , the limit is a conic section, similar to the conic section illustrated in Fig. 4c, whose successive lines $l^{*}_{j}=(P^{I*}_{w0,j},P^{0}_{w0(j+1)})_{(j=-9,..8)}$ are tangents. It can easily be shown that this curve is a parabola. Its equation is obtained from $q^{*}_{j(j=-8,..8)}$ which are the respective intersections of l^{*}_{j} and l^{*}_{j+1}.
2. At the top, above q^{*}_{8}, the limit is the line l^{*}_{8}.
3. In the lower part, below q^{*}_{-8}, the limit is the line l^{*}_{-9}.

The whole valid area on the X_WOZ_W plane can be completed symmetrically to the Z_W-*axis*. To extend the results in the 3D space, the above boundary lines and parabolas defined in the X_wOZ_w plane must be replaced by the respective planes and conic surfaces perpendicular to X_wOZ_w which contain these lines and these parabolas. In addition, the analysis similar to the previous one, wherein we consider the Y_WOZ_W plane allows to delimit the valid area in the 3D space to obtain vertical gaps greater than the threshold α'. The final valid area in the 3D space is the intersection of these two 3D space valid areas.

4. EXPERIMENTAL RESULTS

In this section, we present two types of experiments. The first experiment shows an example of the valid area determination using simulated data. The calibration

segment modeling parameters are set as follows: d_1=850mm, d_0=900mm, $\alpha = \alpha' = 8$ pixels, f=10mm and h=0.003. Fig. 5a illustrates the two computed valid areas ($\alpha = 0$ and α=8) in the $X_W OZ_W$ plane. Then, to validate the final valid area, we have randomly positioned the camera as follows: C_x=-80mm, C_y=60mm and C_z=-10mm. The computed calibration segments are depicted in Fig. 5b. It can be seen that the segments are well separated by rows and by columns. Besides, all the horizontal gaps between consecutive segments are greater than 8 pixels as shown in Fig. 5c. Note that, the vertical gaps are greater than the horizontal gaps because C_y is smaller than C_x.

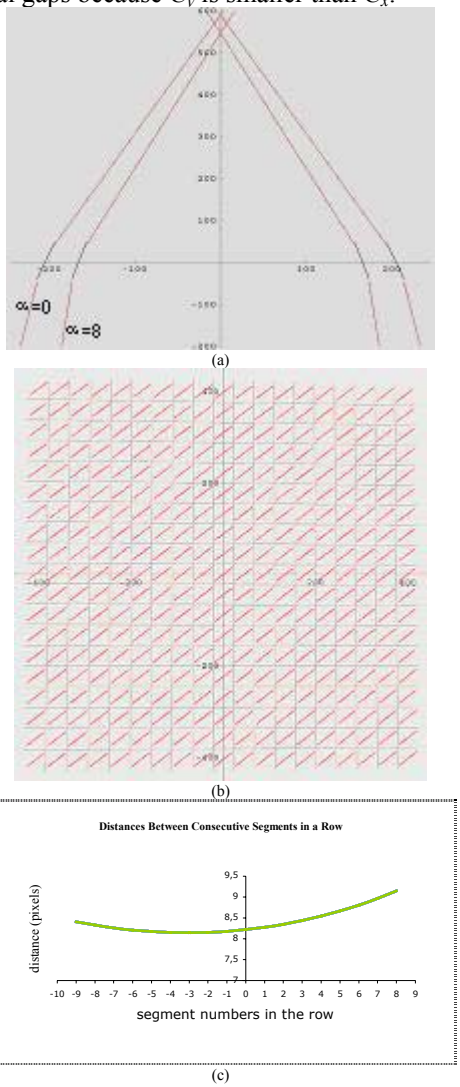

Fig. 5: (a) The computed two valid areas in the $X_W OZ_W$ plane. (b) The calibration segment set obtained from a COS randomly chosen in the final valid area. (b) Plot of horizontal gap between consecutive segments in a row.

The second experiment aims to validate the reliability of the proposed method in real object 3D reconstructions. Two objects are presented: a Chinese vase and a Mask. Figures 6a-c and 7a-c show different images of the two objects. The respective final 3D object reconstructions show that the method yields very accurate results which confirms that the direct correspondence procedure is error free. The complete 3D reconstruction process regardless of the object is achieved in less than 0,1 sec. on a Pentium IV-1.7 *Ghz*. Compared with the GA correspondence method presented in [3], the 3D reconstruction results are exactly identical but the computation time needed is 100 times bigger than the time required by the method proposed in this paper.

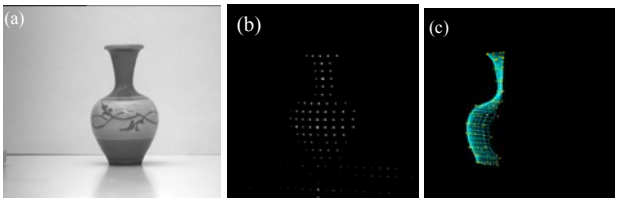

Fig. 6: (a) Gray scale Vase image; (b) The SLS Vase spot image. (c) A B-spline representation of the 3D reconstruction of the Vase.

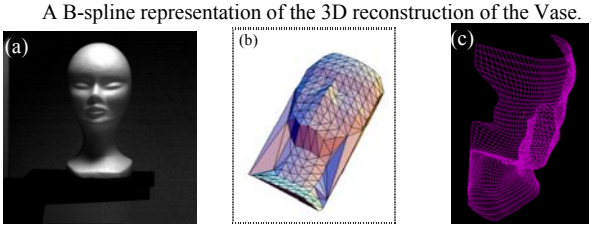

Fig. 7: (a) Gray scale image of the mask; (b) and (c) Triangular meshes and B-spline representations of the Mask 3D reconstruction.

5. CONCLUSION

This paper proposes an original method for automatically obtaining configurations of a Structured Light System which allow to perform an unambiguous direct correspondence in 3D shape reconstruction. Experimental results assess the reliability and the efficiency of the method: 3D objects are reconstructed with high accuracy and a significant time-saving. Definitively, the proposed method provides our SLS with high capabilities to be used in real-time applications.

6. REFERENCES

[1] A. Kiessling, "A Fast Scanning Method for Three-dimensional Scenes", *Proc. 3rd ICPR*, 586-589 (1976)

[2] L. Guisser, R. Payrissat, S. Castan, "PGSD : an Accurate 3D Vision System Using a Projected Grid for Surface descriptions", *Image and Vision Computing 18*, 463-491 (2000)

[3] A. Dipanda, S. Woo, F. Marzani and J.M. Bilbault, "3D Shape Reconstruction in an Active Stereo Vision System Using Genetic Algorithms", *Pattern Recognition 36(9),* 2143-2159 (2003)

[4] F. Marzani, Y. Voisin, L.F.C. Lew Yan Voon and A. Diou, "Calibration of a Three-dimensional Reconstruction System Using a Structured Light Source", *Optical Engineering* 41 (2), 484-492 (2002)

[5] A. Watt and M. Watt, Advanced Animation and Rendering Techniques : Theory and Practice, ACM Press, New York, (1992)